Optimal supercritical potentials for the electron-positron pair-creation rate

J. Unger,[1] S. Dong,[1,2] Q. Su,[1] and R. Grobe[1]

[1]*Intense Laser Physics Theory Unit and Department of Physics, Illinois State University, Normal, Illinois 61790-4560, USA*

[2]*Key Laboratory for Laser Plasmas, School of Physics and Astronomy, Collaborative Innovation Center of IFSA, Shanghai Jiao Tong University, Shanghai 200240, China*

(Received 26 February 2019; published 29 July 2019)

We examine the steady-state electron-positron pair-creation rate for supercritical electric potentials with arbitrary spatial dependence. The numerical optimization algorithms predict that the set of external fields that can maximize the production rate for positrons with a given energy take nontrivial spatial shapes. We explain the underlying physical mechanisms based on a simple analytical model that exploits resonances among the negative energy eigenstates of the Dirac Hamiltonian. The results are rather encouraging from an experimental perspective as they suggest that one does not require unachievable infinitely large fields to maximize the possible pair-creation yield. In fact, in many cases smaller electric fields lead surprisingly to larger yields for given energy ranges.

DOI: 10.1103/PhysRevA.100.012518

I. INTRODUCTION

The possibility to use superstrong external electric or electromagnetic fields to break down the vacuum state and to generate electron-positron pairs is one of the most interesting predictions of quantum electrodynamics [1–5]. It is a fascinating topic of fundamental interest and experimental work to develop high-powered laser systems to confirm this predicted process is presently underway in several laboratories worldwide [6]. It therefore seems obvious that explorations of the optimal space-time profile of the external field to maximize the final particle yield deserve some special attention. The ultimate goal would be to develop a computational algorithm (likely based on infinite-dimensional optimization) to identify the best parameter regime to maximize the particle yield in a given energy range. Some first progress to this goal was recently reported by Kohlfürst *et al.* [7,8] and Hebenstreit and Fillion-Gourdeau [9], who suggested for the first time that the computational framework of the optimal control theory can be utilized to construct the optimal *temporal* dependence of those subgroups of parametrized external fields that are constant in space. These studies were based on the optimization of a few parameters but were recently generalized [10] to allow for arbitrary temporal fields, corresponding to an infinite-dimensional parameter space. In this work, we examine the opposite limit, in which the external field is constant in time, but we construct the optimal *spatial* profile to maximize the steady-state pair-creation rate for particles in a given energy range. These two optimization goals rely on two entirely different pair-creation mechanisms. In the spatially homogeneous case, the electric field's amplitude does not have to be supercritical as the creation mechanism here is based on multi-photon transitions from the initially occupied Dirac sea to positive energy solutions of the Dirac equation [11–14]. In the temporally homogeneous case, the spatial field has to be supercritical, leading to an energy degeneracy as necessary, for example, in the Schwinger decay mechanism of the vacuum [15], which can be interpreted as a tunneling process [16].

Based on recent progress in algorithmic developments [17–24] it has now become possible to extend our knowledge obtained from the finite-dimensional optimization to the more general case of infinite-dimensional optimization. So far, the permitted variation of the external field was described by only two or three parameters, that severely restricted the possible space [25] or time dependence of the external fields.

In this work we apply infinite-dimensional optimization for the spatial dependence of the external field. The preliminary results are surprising and also encouraging. Contrary to what one could have expected from the work with temporal fields, the maximal pair-creation yield is not necessarily associated with singular and technically unachievable limiting cases (such as infinitely narrow fields of infinite amplitudes or infinite energy). In other words, one does not even require any artificial constraints to the search algorithms to avoid these technically undesirable solutions.

The article is organized as follows. In Sec. II we summarize briefly the theoretical framework of the Dirac equation and provide references to prior work about the computational optimization. In Sec. III we provide the spatial shapes of the external fields that optimize the pair-creation yield for a fixed positron energy. In Sec. IV we examine a physical picture based on negaton-quasiresonances that can explain the amplification mechanism. We also introduce a simple two-step model potential that can capture the basic idea of the found amplification mechanism and provides a fully analytical access to the optimization problem. In Sec. V we generalize the prior finding to examine external fields that can optimize the total yield of particles in the entire energy range for the two-step potential. In Sec. VI we return to the numerical infinite-dimensional optimization and construct the spatial form of *the* optimum potential that maximizes the total yield. In Sec. VII we complete the discussion with challenges that can be addressed in future works.

II. OPTIMIZATION ALGORITHM AND THE COMPUTATIONAL IMPLEMENTATION

In this work we calculate the long-time creation rate $\Gamma(E)$ for electron-positron pairs with a desired energy E from the energy eigenstates of the Dirac Hamiltonian. In one spatial dimension (and in atomic units) [26] it takes the form $H = c\sigma_1 p + c^2\sigma_3 + V(x)$, where we assume the coupling to a positron with charge $q = +1$ a.u.; p is the momentum operator and σ_1 and σ_3 denote the 2×2 Pauli matrices. In the external field approximation, the interaction of the vacuum state with the supercritical external potential is given by $V(x)$. For simplicity, we assume that the potential is supercritical and therefore fulfills $V(x \to -\infty) = V_0$ with $V_0 > 2c^2$ and $V(x \to \infty) = 0$.

Following the traditional picture introduced by Dirac, the vacuum is described in this formalism by fully occupied negaton [27] states, which are the eigenstates of $H_0 = c\sigma_1 p + c^2\sigma_3$ with a negative energy less than $-c^2$. In this model system, the supercritical height V_0 can lift the energy of these negaton states for $x \to -\infty$ to positive values ($>c^2$). If these incoming states are transmitted to the right-hand side ($x \to \infty$) (where the potential is zero), then these states change their spinor structure (characteristic of negative energy states of H_0) to the one that is characteristic of positive energy eigenstates. Equivalently, the electric field vector associated with $V(x)$ points on average to the right side. As a result, the created positrons (electrons) are ejected to $x \to \infty$ ($-\infty$) by this force field. The sum of the total probabilities of the (right traveling) transmitted states is 1 minus the vacuum persistence probability. The latter is minimized in this work. Even though it is in principle different and has different units, this quantity can be related to the steady-state particle production rate, which can be computed in quantum electrodynamics in a number of ways [28].

More quantitively, Hund conjectured in 1941 [29] that the field theoretical pair-creation rate per energy $\Gamma(E)$ in the steady state can be computed directly from the quantum mechanical transmission coefficient $T(E)$ associated with the same potential $V(x)$, i.e., $\Gamma(E) = T(E)/(2\pi)$. A rigid mathematical proof for Hund's conjecture and more details about the supercritical pair creation can be found in Ref. [30]. In contrast to the unlimited transmission coefficient for the Klein-Gordon equation (see Refs. [31–33]), the coefficient $T(E)$ for the Hermitian Dirac Hamiltonian is bound between 0 and 1. This means automatically that the resulting pair-creation rate for any positron energy E and *any* potential $V(x)$ cannot exceed the theoretical upper limit of $\Gamma_{\rm lim}(E) = 1/(2\pi)$. For a better interpretation of the data, we purposely separate in our notation the cofactor (2π) in $\Gamma(E)$. The total rate, defined as the energy integral $\gamma \equiv \int dE\Gamma(E)$, where $c^2 < E < V_0 - c^2$, is therefore also naturally bound; i.e., $\gamma_{\rm lim} \equiv (V_0 - 2c^2)/(2\pi)$. It has the units of inverse time, while $\Gamma(E) = d\gamma/dE$ has naturally the units of inverse time and inverse energy.

Unfortunately, there are only a very small number of external potentials known (Sauter potential [34] or stepwise potentials [35]; see below), for which the potential $V(x)$ can be mapped analytically to the corresponding pair-creation rate (or equivalently the transmission coefficient). To determine this rate for potentials with arbitrary spatial shape, numerical methods need to be employed in general.

In this work, we have used techniques such as the iterative QTBM [36] and time-dependent wave-packet scattering methods [37] to guarantee consistent and accurate final data. The acronym QTBM represents the quantum transmission boundary method, which was originally introduced based on the finite difference approximation of the stationary Schrödinger equation on an equidistant grid to simulate electron transport in resonant tunneling diodes. We have generalized it to compute the transmission coefficient for the stationary Dirac equation.

The functional mapping of the potential $V(x)$ to the corresponding rate is given by the functional $\Gamma = \Gamma\{V(x)\}$. This is the key relationship for the optimization program. In order to construct an optimal potential $V_{\rm opt}(x)$ that leads to a maximum pair-creation rate $\Gamma_{\rm opt}(E)$ for a specified positron energy, we have used the steepest ascent [38] and conjugate gradient methods based on Fletcher and Reeves [39] and Polak and Ribiere [40].

In short, in these iterative schemes one starts with an initial guess for $V^{(0)}(x)$, such as the smoothed step function given by the Sauter potential $V^{(0)}(x) = V_0[1 - \tanh(x/w)]/2$. This corresponds to an initial transmission rate $\Gamma^{(0)}(E)$ for a given E. The algorithm determines then numerically the functional gradient $S^{(0)}(x) \equiv \delta\Gamma(E)/\delta V(x)$ for this particular potential $V^{(0)}(x)$, which then acts as a new search direction to find an improved $V^{(1)}(x)$, leading to a larger rate denoted by $\Gamma^{(1)}(E)$. This is accomplished via a line-search $\Gamma = \Gamma\{V^{(0)}(x) + \alpha S^{(0)}(x)\}$ where the search parameter α is constructed to maximize Γ. The resulting new potential $V^{(1)}(x) = V^{(0)}(x) + \alpha S^{(0)}(x)$ serves as the improved potential. This scheme is then repeated until the iteration has converged and $V(x)$ associated with the largest possible rate Γ is obtained.

As the QTBM method is less CPU time consuming than the time-dependent wave-packet scattering method, we have used it in the optimization algorithm to compute Γ. However, in order to examine the accuracy and reliability of this method, we have also employed the slower time-dependent scattering method, which does require the calculation of the wave function.

In our particular case, we found that the algorithm's convergence rate can be increased significantly if the functional derivative is multiplied at each iteration step by a Gaussian window function $W(x)$ centered at $x = 0$. This spatial restriction on the gradient also automatically guaranteed that the potential $V(x)$ for large positive and negative values of x was not modified, as required by the given boundaries $V(x \to -\infty) = V_0$ and $V(x \to \infty) = 0$.

Let us now illustrate the rapid convergence of this iterative scheme. We start with an initial guess of the potential given by $V(x) = V_0[1 - \tanh(x/w)]/2$ with amplitude $V_0 = 2.5c^2$ and spatial turn-on width $w = 0.3/c$. In this case, there are also analytically available expressions for the rate [37] that predict $\Gamma = 0.272/(2\pi)$ for energy $E = 1.25c^2$, which is exactly in the middle of the permitted energy range ($c^2 < E < c^2 - V_0$) of the created positrons, sometimes also called the Klein window.

The spatial axis was discretized between $x = -0.05$ a.u. and $x = 0.05$ a.u. into $N = 2000$ grid points. The algorithm

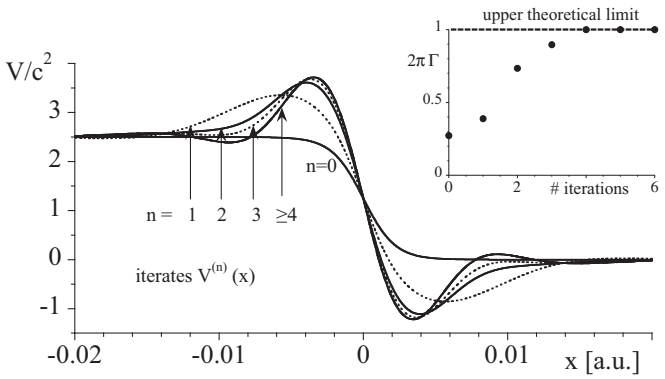

FIG. 1. The first five potentials $V^{(n)}(x)$ to optimize iteratively the pair-creation rate $\Gamma(E)$ for potentials with asymptotic potential height $V(x \to -\infty) = V_0 = 2.5c^2$ and $E = 1.25c^2$. The initial potential was chosen as $V^{(0)}(x) = V_0[1-\tanh(x/w)]$ with $w = 0.3/c$, leading to a starting value of $\Gamma^{(0)} = 0.27/(2\pi)$. The spatial axis was discretized along 2000 grid points with an equidistant spacing $\Delta x = 5 \times 10^{-5}$. As a window function for the functional gradient we used $W(x) = \exp[-(x/0.01)^2]$. In the inset we display the monotonic growth of the associated pair-creation rate $\Gamma^{(n)}(E)$ as a function of the number of iterations n. After only four iterations it becomes very close to its upper theoretically permitted value shown by the dashed line $\Gamma_{\rm lim}(E) = 1/(2\pi)$.

determined the functional derivative $\delta\Gamma(E)/\delta V(x)$ at each of these points. This derivative was then multiplied with the Gaussian window function, given here by $W(x) = \exp[-(x/0.01)^2]$. In Fig. 1 we show the initial Sauter potential and the corresponding sequence of the first four iterated potentials $V^{(n)}(x)$. For $n \geqslant 4$ the spatial profile is converged. In the inset of the figure we show the sequence of improvements to the rate $\Gamma^{(n)}$. Consistent with the data for $V^{(n)}(x)$, we see that in only about four iterations the rate grows from $\Gamma = 0.272/(2\pi)$ to nearly $0.9996/(2\pi)$, which is remarkably close to $\Gamma_{\rm lim}$.

We should finish this section with a brief computational note. From a technical point of view, the infinite-dimensional optimization was realized via the simultaneous optimization of $N = 2000$ independently adjustable parameters. In our case, these parameters were given the magnitudes of the potential at each of the 2000 spatial grid points. We found that this number was sufficiently large to provide numerically converged data while at the same time permitting us to perform the calculations on a Dell PowerEdge R815 system (which has four processors with 16 cores each) within a reasonable CPU time and computer memory. The CPU time associated with the Fletcher-Reeves based conjugate gradient algorithm scales quadratically with the number of required grid points N.

III. COMPUTATIONAL RESULTS FOR THE OPTIMUM FIELDS

We should note that the chosen width of the Gaussian window function determines that spatial range (centered around $x = 0$), in which the potential can be modified by the optimization algorithm. We observed that for a smaller window width the algorithm converged to other potential shapes, that were qualitatively similar to the optimal shown in Fig. 1, but they developed peaks that were narrower and had a much larger amplitude. It is therefore clear that for a given positron energy E there can be several optimum potentials that can lead to a large positron production rate. As all of these potentials predict a value very close to the upper limit, $\Gamma_{\rm lim} = 1/(2\pi)$, the question whether there exists a single global maximum in this infinite-dimensional landscape of functions $V(x)$ is solely of mathematical interest and has not much practical relevance.

The result displayed in Fig. 1 for the optimum $V(x)$ leading nearly to the upper limit of $\Gamma_{\rm lim}(E) = 0.999/(2\pi)$ is interesting. One could have expected that the maximum rate $\Gamma_{\rm opt}$ might be associated with a potential $V(x)$ for which the related electric field [proportional to $-V'(x)$] is largest. This would be given by the abrupt step function $V(x) = V_0\theta(-x)$, where $\theta(x) \equiv (1 + x/|x|)/2$. This expectation is also suggested by the traditional tunneling picture for the Schwinger process, according to which the negatons have to tunnel through the potential step from the left to the right. If this transition region is spatially too extended (i.e., significantly longer than the positron's Compton wavelength $\sim 1/c$), then the transmission (pair-creation rate) is usually negligible. This argument certainly would favor the abrupt potential step to be the best candidate for the largest pair creation.

For this abrupt step $[V_{\rm step}(x) = V_0\theta(-x)]$ one can derive analytically the largest rate (which in this case is always associated with the middle energy $E = V_0/2$) to be $\Gamma(E) = (1 - 4c^4/V_0^2)/(2\pi)$. For our parameter $V_0 = 2.5c^2$, this would amount to $\Gamma(E) = 0.36/(2\pi)$, which consistently exceeds the value $\Gamma(E) = 0.272/(2\pi)$ obtained for the smoother Sauter potential (with $w = 0.3/c$). However, the optimization code did not at all evolve the initial smooth Sauter potential into the expected much sharper function $V_{\rm step}(x)$. In fact, the optimum potential is very smooth and has developed a semioscillatory structure, which then leads to a nearly perfect rate close to $\Gamma_{\rm lim}$, which is about three times larger than the upper limit $0.36/(2\pi)$ provided by the step potential for $V_0 = 2.5c^2$.

In order to examine also other positron energies, we have shown in Fig. 2(a) three potentials, optimized for the chosen energy $E = 1.05c^2$, $1.25c^2$, and $1.45c^2$ and in Fig. 2(b) the corresponding energy dependence of the rate. Quite remarkably, the potential optimized for $1.25c^2$ leads not only to a rate close to the theoretical upper limit $\Gamma_{\rm lim}$ for $E = 1.25c^2$, but also a large rate for a wide range of other energies. In fact, for all energies $1.04c^2 < E < 1.46c^2$ (which is almost the entire Klein range) we find that the rate $\Gamma(E)$ stays above $0.95/(2\pi)$. It might therefore be a perfect candidate to optimize also the total rate γ. (We will further discuss this in Sec. VI below).

The comparison of the data for $E = 1.05c^2$ and $E = 1.45c^2$ reveals an interesting but expected symmetry of $V_{\rm opt}(E)$ as well as of the corresponding rate $\Gamma(E)$. This is related to charge conjugation symmetry between the electronic and positronic formulation of the Hamiltonian. Any potential $V(x)$ for a given positron energy E leads to exactly the same pair-creation rate Γ as its "partner" potential $V_p(x) = -V(-x) + V_0$ and energy $E_p = V_0 - E$. As a result, the rates also have the symmetry $\Gamma_p(E) = \Gamma(V_0 - E)$ as confirmed by the dotted and dashed graphs in Fig. 2(b). From now on we can therefore

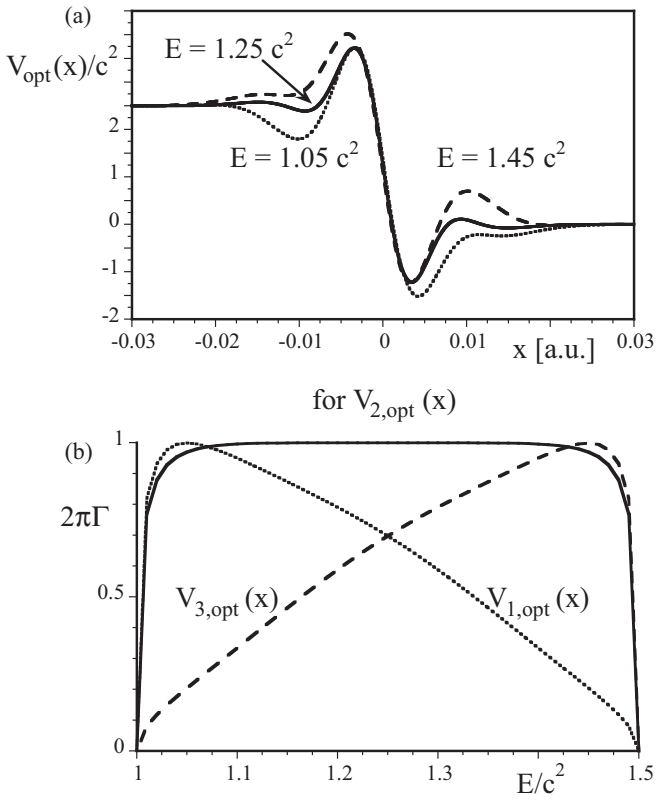

FIG. 2. (a) The spatial profile of three potentials that optimize the pair-creation rate for positrons for chosen final energies $E_1 = 1.05c^2$, $E_2 = 1.25c^2$, and $E_3 = 1.45c^2$. They are denoted by $V_{1,\mathrm{opt}}(x)$, $V_{2,\mathrm{opt}}(x)$, and $V_{3,\mathrm{opt}}(x)$. (b) The general dependence of the pair-creation rate Γ as a function of the energy, calculated for the three optimal potentials $V_{n,\mathrm{opt}}(x)$ with $n = 1, 2, 3$ as shown in (a) [for $V_0 = 2.5c^2$].

restrict our analysis without any loss of generality to positron energies in the smaller range $V_0/2 < E < V_0 - c^2$.

IV. EXPLANATION AND THE MODELING OF THE YIELD AMPLIFICATION MECHANISM

While the complicated optimization algorithm can provide us with numerical information about the possible spatial shapes for the optimal potentials $V_{\mathrm{opt}}(x)$, it would be worthwhile to accompany these purely computational findings also with a better understanding of the underlying physical amplification mechanisms. The numerical analysis provided us with four main findings. First, all data that we have examined for rather wide parameter ranges consistently revealed the development of at least one "bump" on the left side ($x < 0$) of all optimum potentials. Second, the amplitude of these bumps increased with a decrease of their spatial width. Third, the optimum rate is very close to Γ_{lim} and can be achieved for a given energy with potentials that are of *finite* magnitude. Fourth, there is a wide variety of potentials that can lead to the near perfect rate. In this section, we will show that all four of these findings can be explained qualitatively by using a simplified model potential.

In order to crudely model this functional form, we have approximated $V(x)$ by a simple two-step potential, for which we can even obtain a fully analytical mapping from $V(x)$ to the pair-creation rate $\Gamma(E)$. This crude two-step potential is characterized by only two parameters, V and d. It is given by $V(x) \equiv V_0$ for $x < -d$, $V(x) \equiv V$ for $-d < x < 0$, and $V(x) \equiv 0$ for $0 < x$. To better resemble the parameters studied in Secs. II and III, we fixed V_0 at $2.5c^2$ and examine $V_0 < V$. For this potential (and $2c^2 < V$), one can construct analytically the corresponding stationary energy eigenstate for a positive energy E by matching the analytical solution at the boundaries at $x = -d$ and $x = 0$ based on the continuity equation. The resulting analytical expression for the pair-creation rate $\Gamma(E, V, d)$ is given by

$$2\pi\Gamma(E, V, d) = 4c^4 p q_0 {q_1}^2/(N_1 + N_2), \tag{4.1a}$$

where

$$\begin{aligned} N_1 &\equiv c^2 {q_1}^2[(E - c^2)^{1/2}(E_0 - c^2)^{1/2} + (E + c^2)^{1/2}(E_0 + c^2)^{1/2} + c^2]^2\cos^2(q_1 d), \\ N_2 &\equiv \{E_1[(E + c^2)^{1/2}(E_0 - c^2)^{1/2} + (E - c^2)^{1/2}(E_0 + c^2)^{1/2} + c^2] \\ &\quad + c^2[(E + c^2)^{1/2}(E_0 - c^2)^{1/2} - (E - c^2)^{1/2}(E_0 + c^2)^{1/2}]\}^2\sin^2(q_1 d), \end{aligned} \tag{4.1b}$$

and where the three momenta are $p(E) \equiv (E^2 - c^4)^{1/2}/c$, $q_1(E) \equiv [(V - E)^2 - c^4]^{1/2}/c$, and $q_0(E) \equiv [(V_0 - E)^2 - c^4]^{1/2}/c$, and the relevant shifted energies are $E_0 \equiv V_0 - E$ and $E_1 \equiv V - E$.

In Fig. 3 we display this solution $\Gamma(E)$ for $V_0 = 2.5c^2$, $d = 1/c$, and $E = 1.25c^2$ as a function of the "bump" strength V. This potential $V(x, V, d)$ leads to an—at first—rather unexpected behavior of the rate. For example, the rate for $V = 3.23c^2$ amounts to $\Gamma(E) = 0.73/(2\pi)$. This value obviously exceeds the transmission for both the two single-step potentials with height $V_0 = 2.5c^2$ [leading to $\Gamma(E) = 0.36/(2\pi)$] and even $V_0 = 3.23c^2$ [leading to $\Gamma(E) = 0.62/(2\pi)$]. This means that the extra (finite!) bump with amplitude $V = 3.23c^2$ for $-d < x < 0$ and V_0 for $x < -d$ can amplify the pair-creation rate significantly. This is also fully consistent with the more general data shown in Fig. 2(b).

It is also quite remarkable that the transmission does not increase steadily with V; in fact, for $E = 1.25c^2$ and $d = 1/c$ there are other optima for the finite values close to $V_1 = 6.1c^2$, $9.2c^2$, $12.3c^2$, ... This suggests that a resonance mechanism might be responsible for the amplification. The spatial region between two boundaries at $x = -d$ and $x = 0$ could act as some kind of "cavity," in which states with specific wavelengths that fulfill $(n - 1/2)\lambda_n = 2d$ (for $n = 1, 2, 3, \ldots$) naturally could in principle resonate.

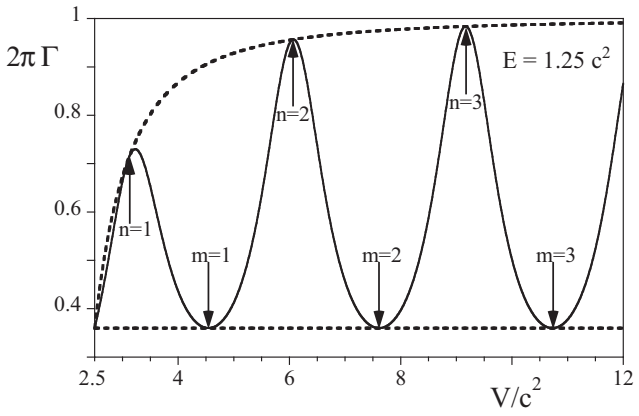

FIG. 3. The pair-creation rate $\Gamma(E)$ associated with the model two-step potential $V(x, V, d)$ as a function of the "bump" strength V for $E = 1.25c^2$ and for $d = 1/c$. The six arrows indicate the predicted values of $V_{\max}$ and $V_{\min}$ according to the resonance condition. The two dashed lines are the envelope solutions according to Eqs. (4.3a) and (4.3b).

We note that this resonance condition for the negaton states should not be confused with the nonrelativistic transmission resonance of quantum mechanical scattering with an attractive well of length d. There a phase shift of π occurs at one of the two boundaries. In this one-dimensional analog of the well-known Ramsauer-Townsend effect the directly reflected and the (after one round trip of length $2d$) reflected waves interfere destructively, leading to the perfect transmission. Correspondingly, in that case the resonance condition is $n\lambda_n = 2d$ (for $n = 1, 2, 3, \ldots$), which are precisely the wavelengths for which the negaton transmission is minimal. This is quite interesting, as the negaton states between $-d < x < 0$ move faster (as $|q_1(E)| > |q_0(E)|$) than the incoming negatons for $x < -d$, which (for usual positive energy states) is characteristic of an attractive well (for $-d < x < 0$).

For a positron energy E, the associated wavelength is $\lambda = 2\pi/q_1(E) = 2\pi c[(V - E)^2 - c^4]^{-1/2}$. For a fixed E and d we can solve this expression for V and we find that the resonant potentials take the values

$$V_{\max} = E + [(n - 1/2)(\pi c/d)^2 + c^4]^{1/2}, \tag{4.2a}$$

$$V_{\min} = E + [(m\pi c/d)^2 + c^4]^{1/2}. \tag{4.2b}$$

For the second equation we have assumed for the wavelengths $m\lambda_m = 2d$ (for $m = 1, 2, \ldots$) such that the pair-creation yield takes a minimum value. We have marked the predicted locations according to Eqs. (4.2a) and (4.2b) for m and $n = 1, 2, 3$ by the six arrows in Fig. 3. Except for the $n = 1$ peak, the agreement is excellent for all n and m values, which shows that this "resonance" mechanism for the wavelength of the negaton states captures indeed the basic characteristics of the amplification and attenuation processes.

On the other hand, we can also use Eqs. (4.1a) and (4.1b) to examine the V dependence of the envelope of the maximum (and also minimum) pair-creation rates at those "resonances," assuming that d was chosen to fulfill the two types of resonance conditions, such that either the cosine or the sine

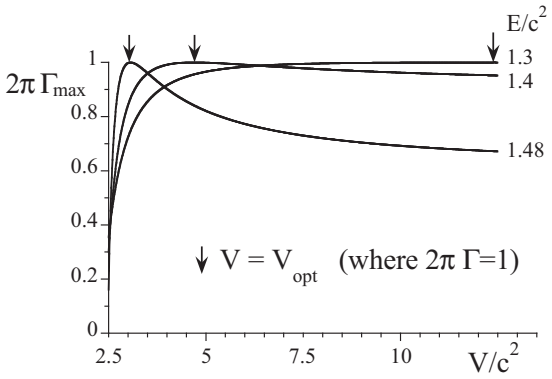

FIG. 4. The envelope solution $\Gamma_{\max}(E, V)$ according to Eqs. (4.3a) and (4.3b) for three positron energies $E = 1.3c^2$, $1.4c^2$, and $1.48c^2$. The arrows point to the locations V_{opt} where the V leads to the perfect (largest theoretically obtainable) pair-creation yield, $\Gamma = \Gamma_{\lim}$.

function in Eq. (4.1b) vanishes. We therefore obtain

$$(2\pi)\Gamma_{\max}(E, V) = 4c^4 pq_0 {q_1}^2/N_2, \tag{4.3a}$$

where $N_2 \equiv \{(E_1+c^2)[(E + c^2)^{1/2}(E_0 - c^2)^{1/2} + (E - c^2)^{1/2}(E_0 + c^2)^{1/2}] + E_1 c^2\}^2$. Similarly, for completeness, we mention the corresponding envelope curve for the minima,

$$(2\pi)\Gamma_{\min}(E, V) = 4c^2 pq_0/N_1, \tag{4.3b}$$

where $N_1 \equiv [(E - c^2)^{1/2}(E_0 - c^2)^{1/2} + (E+c^2)^{1/2}(E_0+c^2)^{1/2} + c^2]^2$. As here the q_1 dependence in the expression for $\Gamma_{\min}(E)$ cancels out and it therefore no longer depends on V; the formula is identical to the Γ for a single step with height V_0. The dashed lines in Fig. 3 display the upper and lower envelopes.

In Fig. 4 we examine the upper envelope function $\Gamma_{\max}(E, V)$ for the optimum rates for three positron energies $E = 1.3c^2$, $1.4c^2$, and $1.48c^2$ according to Eqs. (4.3a) and (4.3b). It turns out that if the positron energy is in the range $V_0/2 < E < V_0 - c^2$ it is always possible to find a particular (finite!) height V (and its width d), such that the pair-creation rate is equal to its theoretically largest possible value $\Gamma_{\lim}$. For better graphical visibility we have marked these locations $V_{\lim}$ ($12.4c^2$, $4.7c^2$, and $3.1c^2$) with the three arrows.

This value for $V_{\lim}$ can be found from the solution Eqs. (4.3a) and (4.3b) if we equate $\Gamma_{\max}$ to $1/(2\pi)$ and solve it numerically for $V_{\lim}$. In Fig. 5 we show the behavior of $V_{\lim}$ as a function of the positron energy. For $E = 1.5c^2$ it approaches $V_{\lim} = V_0$, whereas for $E \to 1.25c^2$ we have $V_{\lim} \to \infty$. We also show the corresponding smallest possible value $d_{\lim}$ at resonance. As d enters the expression for Γ as an argument of a trigonometric function, Γ is always a periodic function of d. But here we focus on the most interesting case with $n = 1$, meaning we examine the smallest value for d.

While the case $V_{\lim} \to \infty$ and $d \to 0$ for $E = 1.25c^2$ is expected, the other limit is quite remarkable. For $V_{\lim} \to 2.5c^2$ and $d \to \infty$ we can actually maintain the perfect rate $\Gamma_{\lim}$. This does not seem to make sense at first as in this limit $V_{\lim}$ is identical to the fixed value of $V_0(=2.5c^2)$ for $x < -d$, such that in this case the resulting $V(x)$ becomes simply a single-step potential, i.e., $V(x) = V_0(1 - x/|x|)/2$. For this easy potential, an analytical solution for $\Gamma(E)$ is available,

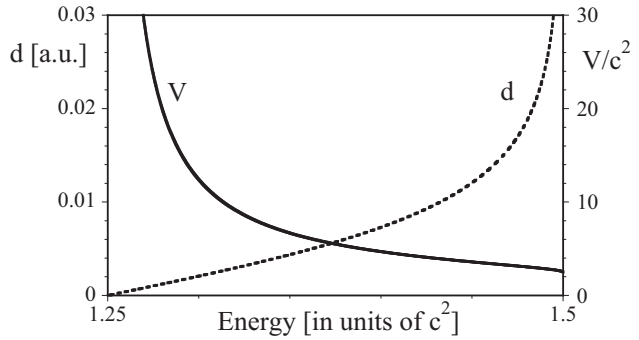

FIG. 5. The perfect amplitude $V_{\rm lim}$ of the potential bump for $-d < x < 0$ as a function of the positron energy E, which leads to a perfect (largest theoretically obtainable) pair-creation yield given by $\Gamma_{\rm lim}$.

which clearly predicts only $\Gamma = 0$ for largest possible energy $E = 1.5c^2$. This means that the two limits of the independent parameters $V \to 2.5c^2$ and $d \to \infty$ do not commute and the order in which they are performed is crucial. It determines which of the two extremum values [0 or $1/(2\pi)$] the pair-creation rate actually takes. This ambiguity is formally reflected in the solution of Eqs. (4.1a) and (4.1b), where the undetermined product $q_1 d$ occurs in the argument of the two trigonometric functions. The limit $V \to 2.5c^2$ corresponds to $q_1 \to 0$ while $d \to \infty$. Only if this product is assumed to approach zero, do we obtain $\Gamma = 0$.

We have omitted an analysis for the positron energies in the lower-energy range $c^2 < E < V_0/2$. Due to the charge conjugation symmetry discussed in Sec. III, the same general conclusions hold also for the lower-energy half of the Klein tunneling regime.

V. OPTIMIZATION OF THE TOTAL YIELD FOR THE MODEL POTENTIAL

Despite its simple form and being characterized by only two parameters (V and d), the two-step potential discussed in Sec. IV seems to capture the basic features of those more general potentials obtained via an infinite-dimensional optimization algorithm. In fact, for any given positron energy, it is always possible to find finite values for V and d to bring the pair-creation value close to the theoretical upper limit $\Gamma_{\rm lim}(E)$. It therefore seems justified to continue to examine this potential also with regard to the optimization of the total rate for all positron energies, defined as $\gamma = \int dE\Gamma(E)$. This rate is naturally also bound from above by $\gamma_{\rm lim} \equiv (V_0 - 2c^2)/(2\pi)$ as shown in Sec. II. It is interesting to examine how close $\gamma_{\rm opt}$, associated with the optimum parameters V and d, can come to $\gamma_{\rm lim}$. While for a given energy E the limit $\Gamma_{\rm lim}(E)$ could be achieved with a finite bump height V, it is not clear at all if $\gamma_{\rm opt}$ can be accomplished similarly with *finite* parameters.

To have two reference values for γ, we note that a single-step potential with $V_0 = 2.5c^2$ leads to $\gamma = 2743/(2\pi)$ which is 71% off from the maximal theoretically possible value $\gamma_{\rm lim} = 9389/(2\pi)$. A single-step potential would theoretically require a gigantic height $V_0 > 74c^2$ such that the associated γ is more than 99% of the corresponding limiting value $\gamma_{\rm lim}$ for this V_0.

In Fig. 6 we have graphed the total pair-creation rate $\gamma(V, d)$ as a function of the two-step potential with parameters V and d. In the numerical range examined, the largest value is about $\gamma_{\rm opt} = 8197/(2\pi)$, which for $V_0 = 2.5c^2$ is only 13% less than the maximal theoretically possible value [$\gamma_{\rm lim} = 9389/(2\pi)$]. This is quite encouraging as it suggests that simple potential shapes can be chosen to bring the total pair production rate close to its upper limit. One could have expected the oscillatory dependence of $\Gamma(E)$ on V and d to be washed out when we integrate Γ over all energies (frequencies); however, the interesting oscillatory structure in $\gamma(V, d)$ shows that this is not true. As the heights along the ring-shaped ridges seem to remain close to $\gamma_{\rm opt}$, there is an infinite manifold of two-step potentials that can optimize the total rate γ.

The location of the sequence of the ridges $\gamma_{\rm ridge}(d, V)$ in the (d, V) plane can be easily derived, if we assume that the most relevant energy E is the center one of the Klein interval, i.e., $E_c \equiv V_0/2$, and use this central value for the resonance-

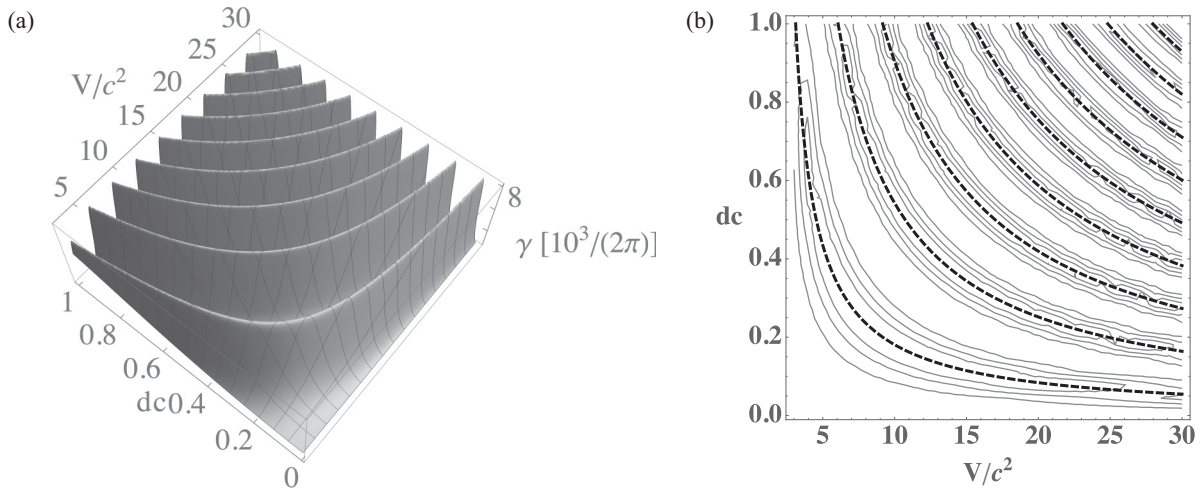

FIG. 6. (a) The total pair-creation rate $\gamma = \int dE\Gamma(E)$ obtained for the two-step potential characterized by a "bump" amplitude V and a bump size d. (b) The corresponding contour plot together with the black dashed lines, given by $d = (n-1/2)\pi c[(V-E)^2 - c^4]^{-1/2}$ for $n = 1, 2 \ldots 9$.

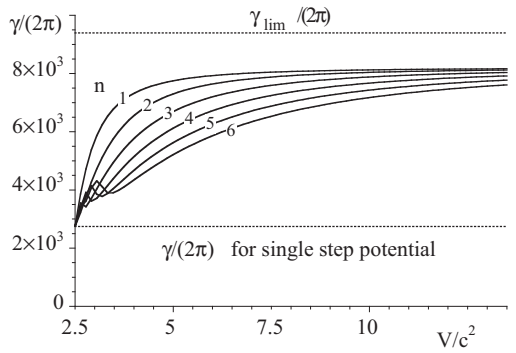

FIG. 7. The magnitude of the pair-creation rate $\gamma = \int dE\Gamma(E)$ along the first six ridges as a function of the potentials "bump" height V for the first six ridges.

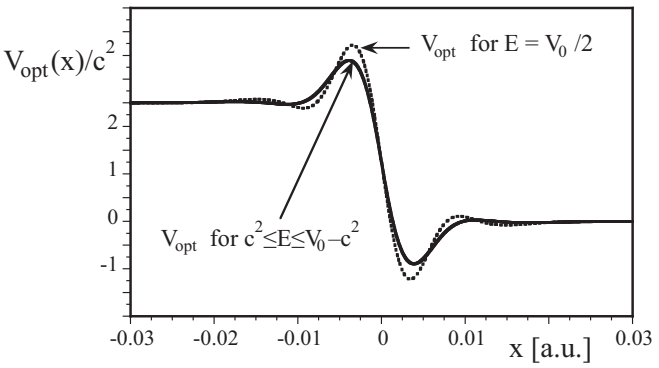

FIG. 8. The optimal potential $V_{\rm opt}$ that maximizes the total electron-positron pair-creation rate $\gamma = \int dE\Gamma(E)$ for all energies in the range $c^2 < E < V_0 - c^2$, with $V_0 = 2.5c^2$. For comparison, we repeat by the dashed line the corresponding potential that optimizes the rate $\Gamma(E)$ for the specific energy $E = 1.25c^2$.

like condition $q_1(E_c)d = (n - 1/2)\pi$. It follows immediately that the ridges (indexed by the integer n) are located on hyperbolas, i.e.,

$$d = (n - 1/2)\pi c[(V - E)^2 - c^4]^{-1/2}. \qquad (5.1)$$

The predicted hyperbolas were superimposed with the dashed lines on the contour plots shown in Fig. 6(b). The agreement with the actual ridges is superb confirming the relevance of the central energy E_c for $\gamma_{\rm ridge}$.

In order to find the absolute maximum value along these ridges, we have replaced this particular energy dependence of E in d in $\gamma = \int dE\Gamma(E)$ and graphed the ridge height as a function of V in Fig. 7 for the first six ridges. While all of these three graphs seem to converge to the same final value for $V \to \infty$, this limiting value, however, is approached rather rapidly. This means that while in principle an infinite value of V is required to reach the precise optimum pair-creation rate γ, a very close value can already be accomplished with *finite* values V.

VI. MOST EFFICIENT POTENTIAL $V_{\rm opt}(x)$ BASED ON INFINITE-DIMENSIONAL OPTIMIZATION

In this section we show that the major findings based on the simple two-step potential are of relevance even for the most general space of arbitrary potentials $V(x)$, that are only constrained by the required boundary condition, $V(x \to -\infty) = V_0$ and $V(x \to \infty) = 0$.

From a computational perspective, the same computational methodology that was used to construct the optimal potential for a given positron energy E can be exploited to calculate $V(x)$ that maximizes the total yield. In the required functional mapping of the potential $V(x)$ to the corresponding rate $\gamma = \int dE\Gamma(E)$ we have discretized the energy space between the two limits $E = c^2$ and $E = V_0 - c^2$ into 200 discrete energies and replaced the integration by a discrete sum (trapezoidal rule) over all energies. As the integrand $\Gamma(E)$ turned out to be not very oscillatory, simulations with 100 and 200 energies led to the same result. As the functional gradient needed to be computed numerically for each of the 2000 spatial grid points, due to this energy summation, the required CPU to maximize γ was 200 times longer than required for $\Gamma(E)$.

In Fig. 8 we present the optimal potential $V_{\rm opt}(x)$ for $V_0 = 2.5c^2$. It shows a striking similarity to the corresponding potential that maximized the rate for the single energy $E = 1.25c^2$, which is exactly halfway in the Klein range. This finding is not so completely unexpected as we have noted in Fig. 2(a) already a certain commonality among the amplitudes and spatial shapes of the potentials $V_{\rm opt}(x)$ that optimized the rates Γ for three rather different energies within the Klein range.

This finding is also fully consistent with the recently reported superposition principle for the simultaneous optimization (SPSO) for collective responses [41]. In this case, the dynamics of sets of independent systems were examined, which were simultaneously coupled to the same time-dependent external force. Using optimal control theory, it was shown that the most efficient temporal pulse shape for this force that can maximize simultaneously the collective response of these systems can be related to the individual forces that would optimize each system separately.

In this sense, the present system confirms qualitatively that the SPSO, which was originally derived only for temporal systems, can likely be generalized to spatial optimizations as well. But, of course, more detailed studies are required.

We should finish with a note about the magnitude of the total pair-creation rate γ associated with *the* optimal potential. We calculated the numerical value $\gamma_{\rm opt} = 9083/(2\pi)$, which is only 3.26% less than the upper limit of the maximal theoretically possible value $[\gamma_{\rm lim} = 9389/(2\pi)]$. We should point out that the derivation of $\gamma_{\rm lim}$ assumed that $T(E) = 1/(2\pi)$ for the entire Klein range of all energies. However, the numerically found (best possible realizable choice of the) potential shows that for any finite V_0 (such as $V_0 = 2.5c^2$ as in our case), the assumption of an energy-independent $\Gamma(E)$ is not realizable by any potential. In fact, one can show that at the smallest and largest positron energies we usually have vanishing rates; i.e., $\Gamma(E = c^2) = \Gamma(E = V_0 - c^2) = 0$. This means that the present numerical data obtained for $V_{\rm opt}(x)$ suggest that the true (and actually achievable) largest rate is not $\gamma_{\rm lim}$ but actually $\gamma_{\rm opt}$, which still exceeds the rate from a simple step potential $[\gamma = 2743/(2\pi)]$ by 71%.

VII. SUMMARY AND OPEN QUESTIONS

Complementary to recent studies in which the temporal profiles of spatially homogeneous electric field pulses were optimized [7–10], in this work we have examined fields that are temporally constant but vary in space. For a single-step potential, given, for example, by Sauter's tanh potential, the theoretically maximum pair-creation rate $\Gamma_{\rm lim}$ can be reached only in the technically unachievable limit of $V_0 \to \infty$. However, with an alternative spatial profile one can obtain this desirable upper limit for a *finite* potential height. We view this exciting observation as the most important finding of this infinite-dimensional optimization. There is also a clear message for the distribution in the corresponding electric field configuration. The steady-state pair-creation rate can apparently be amplified significantly if the field energy is not necessarily concentrated onto a small domain in space. It is more advisable to distribute this energy along several spatial domains in order to achieve the advantageous resonance conditions. This conclusion even holds if the total pair-creation rate (for all positron energies) needs to be maximized.

In view of the extremely short timescales of the order of 10^{-21} s that are characteristic of the pair-creation process, this steady field assumption might not be so unphysical as the experimental fields might vary temporally on significantly longer timescales, such that the steady-state situation assumed in this work could be reasonable. However, as the pair-creation process can be triggered simultaneously by the supercritical strength as well as the rapid temporal variation of the external electromagnetic environment, future theoretical optimization study that could maximize the particle yield for a field with arbitrary space-time dependence would be ideal. While optimal control theory has led to significant algorithmic improvements in a wide variety of research areas, there has not been sufficient study of a theoretical approach that could optimize simultaneously the spatial and temporal dependence of a control force field.

In contrast to the prior studies of spatially homogeneous fields, where limitations on the amplitude or energy of the fields had to be imposed as external constraints to avoid undesirable fields with infinite parameters, the present study revealed that the maximum theoretically achievable pair-creation rate for a given final positron energy (associated with a transmission coefficient equal to unity) can be accomplished in fact with *finite* fields and therefore possibly technically achievable parameters. This rather encouraging finding certainly raises the hope that similarly *finite* space-time parameters can lead to an optimum pair creation.

The necessity to examine the full space-time dependence will also permit us to include the potentially relevant effects associated with the magnetic field component of the radiation pulse, that were shown to trigger an amplifying as well as attenuation impact on the pair-creation yield [42] depending on the spatial orientation and other geometrical configurations.

The possibility to exploit resonances to amplify the pair-creation rate is, of course, not a new concept in itself. For example, in the case of temporally homogeneous fields, Fillion-Gourdeau *et al.* [43] have shown that laser-induced bound states can effectively increase the transfer rate between the lower- and upper-energy continuum states in diatomic molecules. Also, recently, a possible enhancement as well as a suppression of certain positron energies due to the presence of an additional localized field was proposed in [44,45].

While we are still in the cradle stages of our theoretical understanding, it is our hope that the present study can motivate further investigations with the ultimate goal to become really useful to guide potential experiments.

ACKNOWLEDGMENTS

S.D. would like to thank ILP for the nice hospitality during his visit to Illinois State and acknowledges the China Scholarship Council program. This work has been supported by the NSF, NSFC (Grants No. 11529402 and No. 11721091) and Research Corporation.

[1] W. Greiner, B. Müller, and J. Rafelski, *Quantum Electrodynamics of Strong Fields* (Springer-Verlag, Berlin, 1985).

[2] A. A. Grib, S. G. Mamaev, and V. M. Mostepanenko, *Vacuum Quantum Effects in Strong Fields* (Atomizdat, Moscow, 1988), republished by Friedmann Laboratory, St. Petersburg (1994).

[3] E. S. Fradkin, D. M. Gitman, and Sh. M. Shvartsman, *Quantum Electrodynamics with Unstable Vacuum* (Springer-Verlag, Berlin, 1991).

[4] For a comprehensive review, see, e.g., A. Di Piazza, C. Müller, K. Z. Hatsagortsyan, and C. H. Keitel, Rev. Mod. Phys. **84**, 1177 (2012).

[5] For a more recent review, see, B. S. Xie, Z. L. Li, and S. Tang, Matter Radiat. Extremes **2**, 225 (2017).

[6] For recent advances in high-power laser systems, see, for example, the websites of the following labs: ELI (Paris); diocles (Lincoln); xfel (Hamburg); sparc (Darmstadt); Vulcan, HiPER, and Astra Gemini (Oxfordshire); polaris (Jena) or Shenguang III (Mianyang); LCLS (Stanford); TPL (Austin); or numerous references in https://eli-laser.eu/.

[7] C. Kohlfürst, Master's thesis, Graz University, arXiv:1212.0880.

[8] C. Kohlfürst, M. Mitter, G. von Winckel, F. Hebenstreit, and R. Alkofer, Phys. Rev. D **88**, 045028 (2013).

[9] F. Hebenstreit and F. Fillion-Gourdeau, Phys. Lett. B **739**, 189 (2014).

[10] J. Unger, S. S. Dong, R. Flores, Q. Su, and R. Grobe, Phys. Rev. A **99**, 022128 (2019).

[11] N. B. Narozhny and A. I. Nikishov, Sov. J. Nucl. Phys. **11**, 596 (1970).

[12] E. Brezin and C. Itzykson, Phys. Rev. D **2**, 1191 (1970).

[13] V. S. Popov, JETP Lett. **13**, 185 (1971) [Sov. Phys. JETP **34**, 709 (1972)].

[14] W. Y. Wu, F. He, R. Grobe, and Q. Su, J. Opt. Soc. Am. B **32**, 2009 (2015).

[15] J. S. Schwinger, Phys. Rev. **82**, 664 (1951).
[16] S. R. Coleman, Nucl. Phys. B **298**, 178 (1988).
[17] D. E. Kirk, *Optimal Control Theory: An Introduction* (Prentice-Hall, Englewood Cliffs, NJ, 1970).
[18] R. Dechter, *Constraint Processing* (Morgan Kaufmann, Burlington, MA, 2003).
[19] D. S. Naidu, *Optimal Control Systems* (CRC Press, Baca Raton, FL, 2003).
[20] J. J. Leader, *Numerical Analysis and Scientific Computation* (Addison Wesley, Boston, 2004).
[21] R. Battiti, M. Brunato, and F. Mascia, *Reactive Search and Intelligent Optimization* (Springer-Verlag, Heidelberg, 2008).
[22] W. Sun and Y. X. Yuan, *Optimization Theory and Methods: Nonlinear Programming* (Springer-Verlag, Heidelberg, 2010).
[23] A. Gosavi, *Simulation-Based Optimization* (Springer-Verlag, Heidelberg, 2015).
[24] D. Bertsekas, *Dynamic Programming and Optimal Control* (Athena Scientific, Belmont, MA, 2017).
[25] S. S. Dong, M. Chen, Q. Su and R. Grobe, Phys. Rev. A **96**, 032120 (2017).
[26] T. Cheng, Q. Su, and R. Grobe, Contemp. Phys. **51**, 315 (2010).
[27] Z. Bialnicki-Birula and Z. Bialynicka-Birula, *Quantum Electrodynamics* (Pergamon Press, Oxford, 1975); the term negaton was also used in J. M. Jauch and F. Rohrlich, *Theory of Photons and Electrons* (Springer-Verlag, Berlin, 1976).
[28] A. I. Nikishov, Nucl. Phys. B **21**, 346 (1970); T. D. Cohen and D. A. McGady, Phys. Rev. D **78**, 036008 (2008); L. Labun and J. Rafelski, *ibid.* **79**, 057901 (2009); S.-P. Kim and D. Page, arXiv:1904.09749 [hep-th].
[29] F. Hund, Z. Phys. **117**, 1 (1941).
[30] Q. Z. Lv, S. Dong, C. Lisowski, R. Pelphrey, Y. T. Li, Q. Su, and R. Grobe, Phys. Rev. A **97**, 053416 (2018).
[31] T. Cheng, M. R. Ware, Q. Su, and R. Grobe, Phys. Rev. A **80**, 062105 (2009).
[32] R. E. Wagner, M. R. Ware, Q. Su, and R. Grobe, Phys. Rev. A **81**, 052104 (2010).
[33] Q. Z. Lv, H. Bauke, Q. Su, C. H. Keitel, and R. Grobe, Phys. Rev. A **93**, 012119 (2016).
[34] F. Sauter, Z. Phys. **69**, 742 (1931).
[35] M. Jiang, W. Su, X. Lu, Z. M. Sheng, Y. T. Li, Y. J. Li, J. Zhang, R. Grobe, and Q. Su, Phys. Rev. A **83**, 053402 (2011).
[36] C. S. Lent and D. J. Kirkner, J. Appl. Phys. **67**, 6353 (1990). For a generalization of the QTBM to relativistic systems, see Q. Z. Lv, A. C. Su, M. Jiang, Y. J. Li, R. Grobe, and Q. Su, Phys. Rev. A **87**, 023416 (2013).
[37] J. W. Braun, Q. Su, and R. Grobe, Phys. Rev. A **59**, 604 (1999).
[38] W. H. Press, S. A. Teukolsky, W. T. Vetterling, and B. P. Flannery, *Numerical Recipes in C: The Art of Scientific Computing*, 2nd ed. (Cambridge University Press, New York, 1992).
[39] R. Fletcher and C. M. Reeves, Comput. J. **7**, 149 (1964).
[40] E. Polak and G. Ribière, Rev. Fr. Inf. Rech. Oper. **3**(16), 35 (1969).
[41] S. Dong, R. Flores, J. Unger, Q. Su, and R. Grobe, Phys. Rev. E **98**, 012221 (2018).
[42] Q. Z. Lv, S. Dong, Y. T. Li, Z. M. Sheng, Q. Su, and R. Grobe, Phys. Rev. A **97**, 022515 (2018).
[43] F. Fillion-Gourdeau, E. Lorin, and A. D. Bandrauk, Phys. Rev. Lett. **110**, 013002 (2013).
[44] Q. Z. Lv, Q. Su, and R. Grobe, Phys. Rev. Lett. **121**, 183606 (2018).
[45] Q. Su and R. Grobe, Phys. Rev. Lett. **122**, 023603 (2019).